# CMOS pixels crosstalk mapping and its influence on measurements accuracy for space applications

M.Estribeau*, P.Magnan**

SUPAERO – Integrated Image Sensors Laboratory
10 avenue Edouard Belin, 31400 Toulouse, France

## ABSTRACT

Due to different local intra-pixel sensitivity and crosstalk between neighboring pixels, the Pixel Response Function of detectors (PRF - signal of the pixel as a function of a point source position) is generally non-uniform. This may causes problems in space application such as aperture photometry and astrometry (centroiding). For imaging applications, an important crosstalk yields to a loss of resolution, i.e. a poor image quality, commonly quantified by the Modulation Transfer Function (MTF). So, crosstalk study is of primary importance for our applications.
A dedicated test chip (using a technology optimized for imaging applications) has been developed in order to get both MTF data and influence of the various areas of the pixel to its own response and the one of its neighbors. The results obtained with pixel kernels and direct MTF measurements, performed on the same chip at different wavelengths, are analyzed and compared in order to correlate them. So it is possible to draw conclusions -that can be applied at the design level - allowing to get a better MTF and to minimize errors on aperture photometry and centroiding computation.

**Keywords :** APS, space, CMOS, cameras, Image Sensor.

## 1. INTRODUCTION

Crosstalk in an image sensor results from photo-generated carriers having the possibility to diffuse and to be collected by a neighboring pixel. It occurs in both monochrome and color image sensors. In this last case, crosstalk makes poor color separation and its reduction may avoid color mixing.

Our study focuses on monochrome CMOS Image Sensors crosstalk behavior. For sensing and pointing applications, an important crosstalk may affect centroiding determination accuracy. For imaging applications, it yields to a loss of resolution, i.e. a poor image quality, commonly quantified by the Modulation Transfer Function (MTF). So, crosstalk study is of primary importance for our applications.

Due to its use in high volume low cost applications, CMOS image sensors suffer from the reputation of yielding a limited image quality and sensitivity (compared to CCDs), which may be problematic for space applications measurement accuracy. But thanks to efforts made at the foundry level, optimized CMOS photodiode are nowadays available (figure 1). More, they have others advantages that make them suitable for space applications. Access to a chosen region of interest of the entire array is possible thanks to the random access of pixels. In addition CMOS image sensors offers better radiation tolerance (to ionizing radiations, but also to protons and heavy ions) than CCDs.

* magali.estribeau@supaero.fr; phone +33 5 62 17 82 96; fax +33 5 62 17 83 45
** pierre.magnan@supaero.fr; phone +33 5 62 17 80 79; fax +33 5 62 17 83 45

The effects of non-uniform response (including crosstalk) on astronomical measurements accuracy have already been studied in the case of CCDs [1]. In CMOS sensors, presence of the transistors area (figure 2) can affect the spatial response of the pixel which may be crucial for space applications.

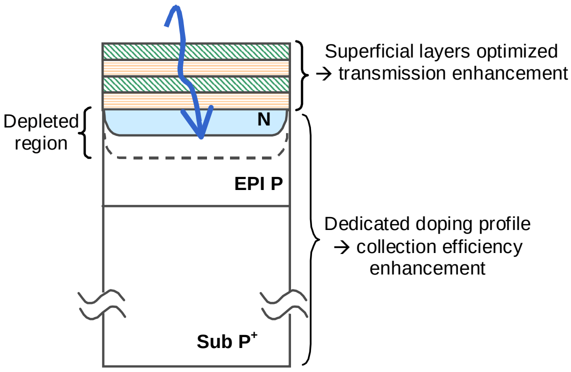


Figure 1. Schematic cross-section of a photodiode

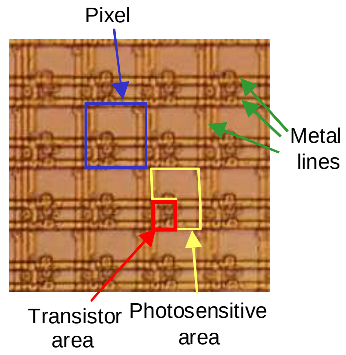


Figure 2. Typical view of CMOS pixels

We had the opportunity to develop sensors using a 0.35µm CMOS optimized technology, thus allowing expecting good performances for imagery applications. We have made, on the same type of pixels, quantum efficiency, crosstalk and MTF measurements. This work allows us to bring up some conclusions about the way to optimize pixels for space applications such as astrometry, centroiding and imagery.

## 2. ASTRONOMICAL MEASUREMENTS ACCURACY

### 2.1. Pixel Response Function

According to the definition of D.Kavaldjiev and Z.Ninkov [2], the Pixel Response Function (PRF) is defined as the signal detected by a pixel when this one and its neighbors are scanned by a point source (infinitesimally small). So, PRF is a spatial map of the intra-pixel sensitivity but also of the crosstalk. Considering that $PSF_0(x,y)$ is the PSF of the optics (image formed on the detector surface) centered on (x,y), the pixel (n,m) response s(n,m;x,y) is obtained by [3]:

$$s(n, m; x, y) = PSF_0(x, y) * PRF(n, m; x, y)$$

We remind that the MTF is relied to PRF by :

$$MTF(\nu_x, \nu_y) = \left|FT[PRF(x, y)]\right|$$

where FT denotes the two-dimensional Fourier Transform. Ideally, the PRF should be uniform within the pixel boundaries (i.e. uniform pixel sensitivity) and zero outside (i.e. no crosstalk). In point of fact, intra-pixel sensitivity presents variations due to transmittance non-uniformity and collection efficiency spatial variations. More, optical and diffusion crosstalk yield to a non-zero PRF outside the pixel boundaries, thus having a direct effect on MTF and so on image quality : the higher is the crosstalk (generally increasing with wavelength), the poorer is the MTF.

### 2.2. Influence of non-uniform PRF on measurements accuracy

In aperture photometry, the total energy received from a star is measured by the summation of the detected signal within an aperture. The aperture photometric signal S can be written as the summation of the pixels values s(n,m) within the defined aperture :

$$S = \sum_{n,m} s(n, m)$$

The photometric signal dependence on the image position can be quantified by defining a shift error $\sigma_{photo}$ , defined as the standard deviation of the photometric signal S, normalized by the average signal $S_{av}$ :

$$\sigma_{photo} = \frac{std(S)}{S_{av}}$$

In the case of a uniform PRF, S does not depend on the image position within the pixel and the photometric shift error $\sigma_{shift}$ will always be zero. However, the positional shift error in centroiding computations $\sigma_{position}$ will always be greater than zero, even if the PRF is ideal. The photometric shift error is defined as follow :

$$\sigma_{position} = std(D)$$

where D is the distance between the center coordinates $(x_0,y_0)$ of the input star and the computed centers $(x_c,y_c)$:

$$D = \sqrt{(x_c - x_0)^2 + (y_c - y_0)^2} \quad \text{with} \quad x_c = \frac{\sum_{n,m} s(n,m)x}{\sum_{n,m} s(n,m)} \quad \& \quad y_c = \frac{\sum_{n,m} s(n,m)y}{\sum_{n,m} s(n,m)}$$

The figures 3 and 4 represent D and $\sigma_{position}$ obtained when considering a uniform PRF and a gaussian input PSF with a variable FWHM (full width at the half maximum). We can see on figure 4 that the error is significant in the case of undersampled image.

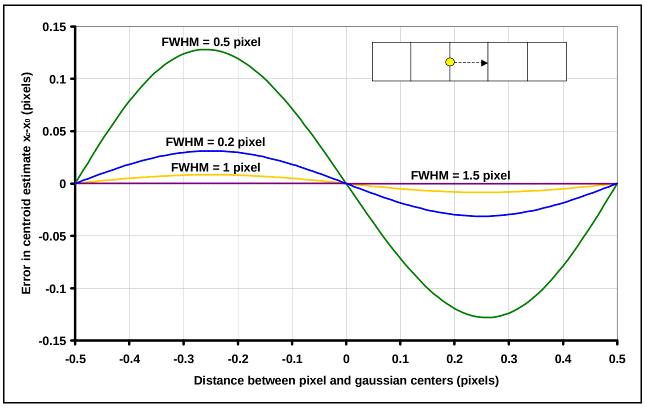


Figure 3. Error in centroid estimate as function of the PSF center for a gaussian PSF and a uniform PRF

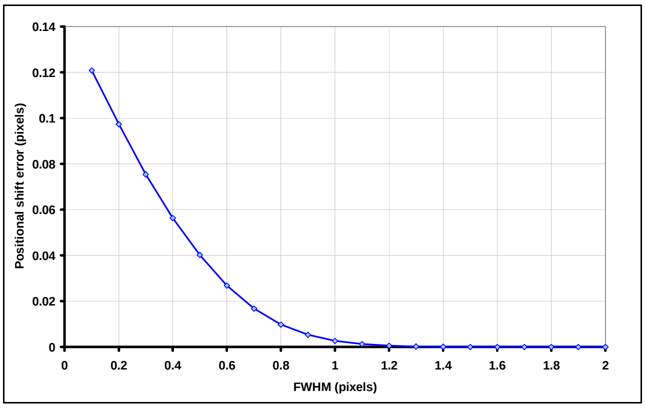


Figure 4. Positional shift error as function of FWHM for a gaussian PSF and a uniform PRF

Studies have been made on CCD pixels in the case of front-side and back-side illumination [2][1]. By measuring precisely the PRF of both types of pixels for several wavelengths, the authors were able to compute the astronomical measurement accuracy with these real PRF. They compared them with the results obtained with an ideal (uniform) PRF. Their conclusion is that a non-uniform PRF contributes to uncertainty in astronomical measurements. More, a back-side illuminated CCD show better performances than a front-side illuminated CCD due to the fact that its PRF is more uniform. However, in both cases, errors in centroid computation increase with wavelengths.

As for CCDs, CMOS PRF are non-uniform and wavelength dependent. So, we have developed a test chip dedicated to intra-pixel sensitivity and crosstalk analysis, but also to MTF measurements.

# 3. CHIP DESCRIPTION

## 3.1. Overall description

The test chip consists in an array of 128x128 photodiodes pixels, 13-µm pitch. It uses a 0.35µm technology optimized for imaging applications, thus theoretically yielding to a collection efficiency improvement and low crosstalk so good performances in terms of Modulation Transfer Function. The pixels (figure 5) have been designed to use only two metal layers (M1 and M2) leaving the upper metal layer (M3) available for light shielding purpose (figure 6).

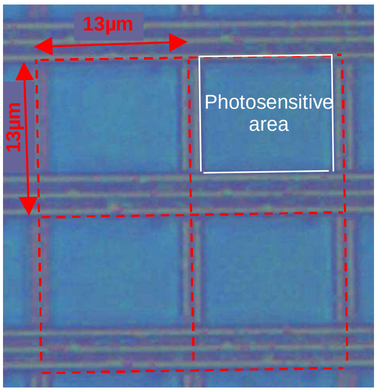


Figure 5 : Photograph of 2x2 pixels

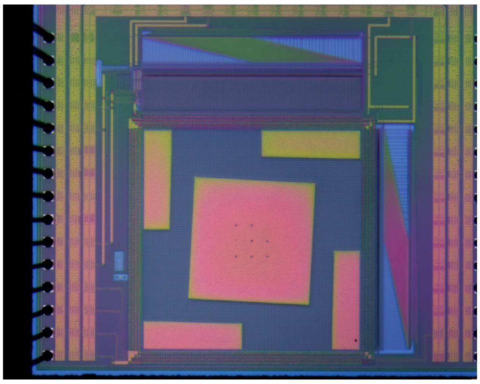

Figure 6 : Photograph of the chip

Initially, the chip has been designed in order to get easily MTF results. For that we have implemented on-chip metal patterns ; a large metal block emulates the slanted-edge pattern for providing MTF data using the ISO 12233 methodology [4]. As only the borders of the metal block are used for MTF measurements, pixels located in the center of this block may be used for additional characterizations. Thirteen of them (numbered 1-13 and called test pixels), have been kept totally or partially unmasked (figure 7). By measuring the quantum efficiency of these pixels, we can evaluate the variations of local sensitivity. More, by analyzing the responses of their neighbors, an evaluation of the contribution of each part of the pixel to the surrounding pixels signal (crosstalk) is possible.

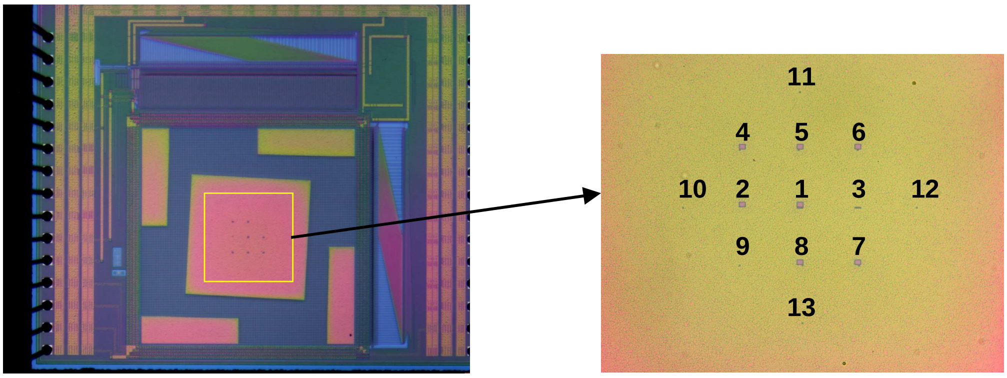


Figure 7 : Photograph of the test pixels

The first step of the characterization was to quantify the M3 optical transmission and the conversion gain (CVF) of the metal-covered pixels. Since the responses of the masked pixels do not show a significant increase with regard to the illumination, we can consider that the optical transmission is negligible and even zero. It is then possible to use a uniform illumination for the crosstalk evaluation. Due to the use of a metal layer sufficiently high, differences between measured CVF values are negligible so the numerical response of each pixel does not need to be corrected of its own CVF.

### 3.2. Test pixels description

For our study, we have focused attention on 3x3 pixel kernels containing test pixels n°1, n°2 and n°9 to n°13 (figure 8). The test pixels n°1 is totally uncovered and may be considered as a reference pixel. The transistors area of the test pixel n°2 is totally covered while the pixels n°9 to n°13 are totally covered except a little part (about 7µm²) of the transistors area.

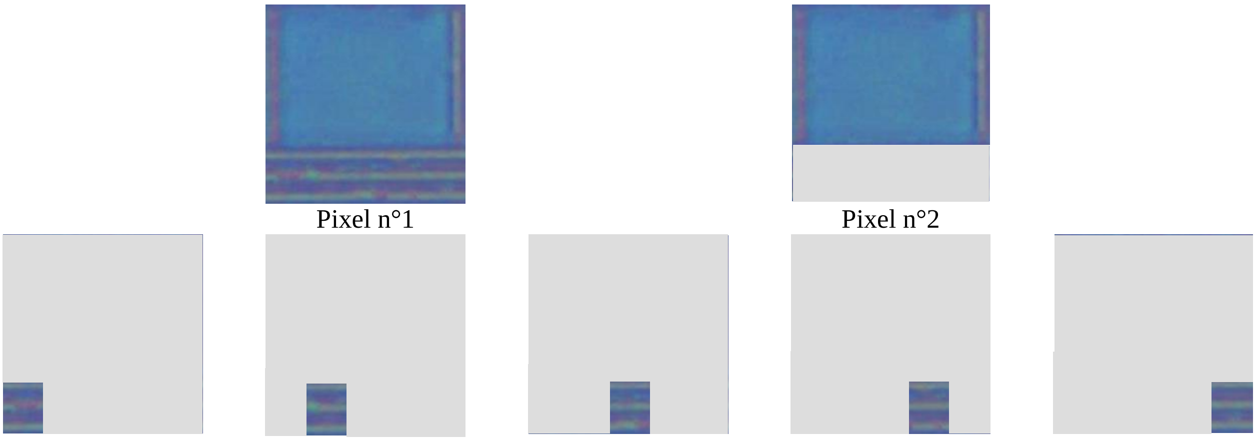


Figure 8 : Photograph of test pixels used for QE and crosstalk evaluations

## 4. ELECTRO-OPTICAL MEASUREMENTS

### 4.1. Quantum efficiency

Measurements of quantum efficiency have been made using a monochromator. Thus allows us to explore the spectral range 400-900mn with a 10 nm step. Results obtained for the pixels n°1 and n°2 are shown on the figure 9.

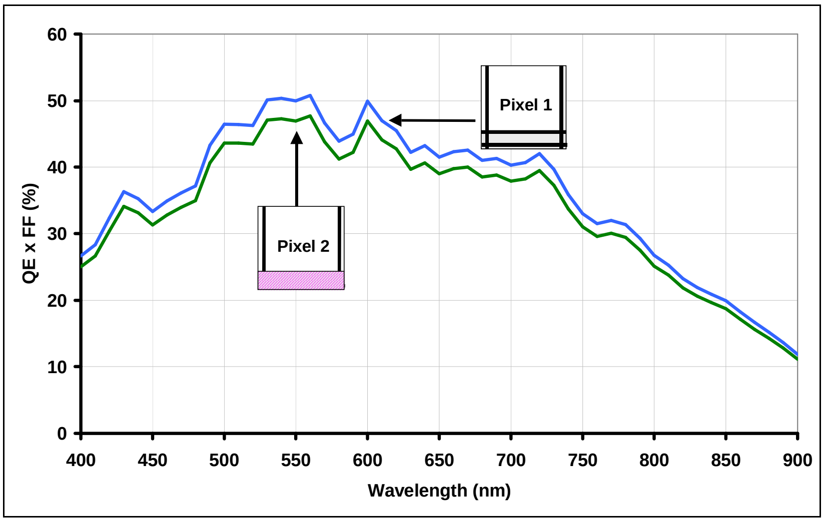


Figure 9: Transistors area masking influence on quantum efficiency

As expecting with an optimized technology, quantum efficiency (QE) results are good. Peak quantum efficiency of the reference pixel (pixel n°1) is obtained at the wavelength of 560nm (QE x FF = 51%). The sensor also demonstrates good response in blue and red, thus proving really good performance in photon transmission and collection efficiency. Another important conclusion that can be seen on these curves is the transistors area masking influence. The pixel n°2 QE is slightly lower than the pixel n°1 QE ; so we can deduce that carriers are generated in the transistors area, diffuse to the depletion region and participate to the pixel response.

The contribution to the overall photo-response of each part of the transistors area can be compared by examining the relative quantum efficiency of pixels n°9 to n°13. Results shown in figure 10 demonstrate a very non-identical contribution.

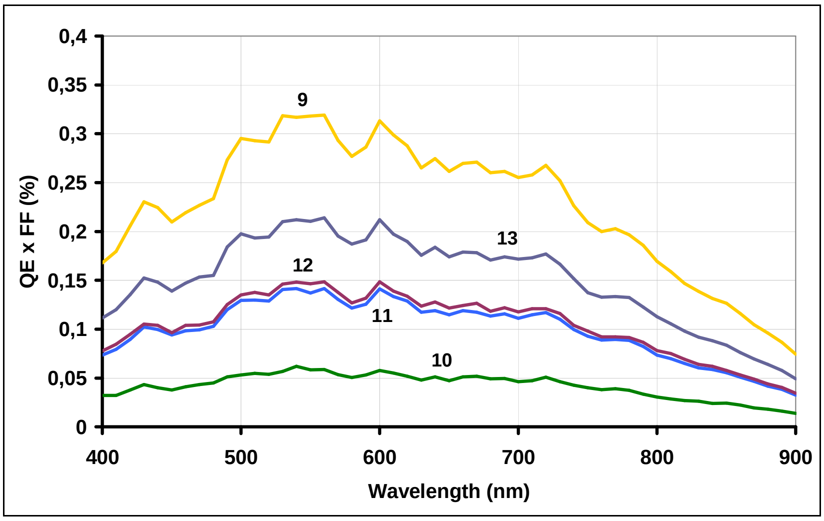


Figure 10 : Transistors area contribution in quantum efficiency

In a first approximation, these differences in term of quantum efficiency may be explained by the non-uniformity of the superficial layers transmittance. Transistors area contains metal lines and transistors and, due to the use of silicides, only parts containing no N diffusion, polysilicon or metal lines are really tranmissive. Differences in charge collection efficiencies must also be taken into account to explain QE differences but this point will be explain more precisely in the next part. As a conclusion, the PRF observed inside the pixel boundaries is, as for CCD, non-uniform.

### 4.2. Crosstalk analyzis

Considering a 3x3 pixels kernel with a test pixel in its center, only this one can receive illumination. The surrounding pixels are called according to their position with respect to the central one (figure 11).

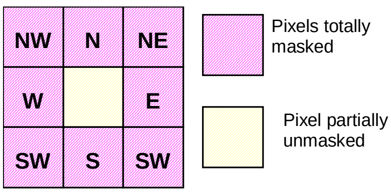


Figure 11 : Denomination of the pixels for crosstalk study

We measure the signal with regard to the source luminance for each pixel of the kernels, and calculate the ratio between the slope of the masked pixels against the central one (totally or partially unmasked). So we can evaluate the quantity of charges generated in the central pixel and diffusing to the neighbors ones, i.e. the crosstalk.

Let us consider the block containing the pixel n°1, which one is totally uncovered. The block relative responses, obtained at 500nm and 800nm, are respectively represented on the figures 12 and 13.

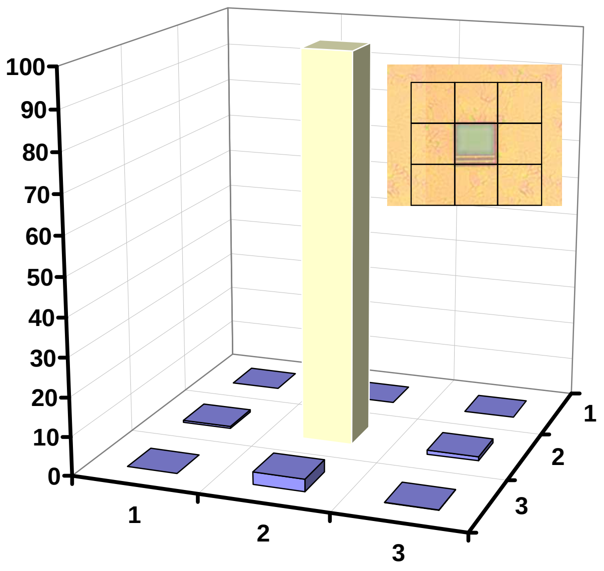


Figure 12 : Block response at 500nm

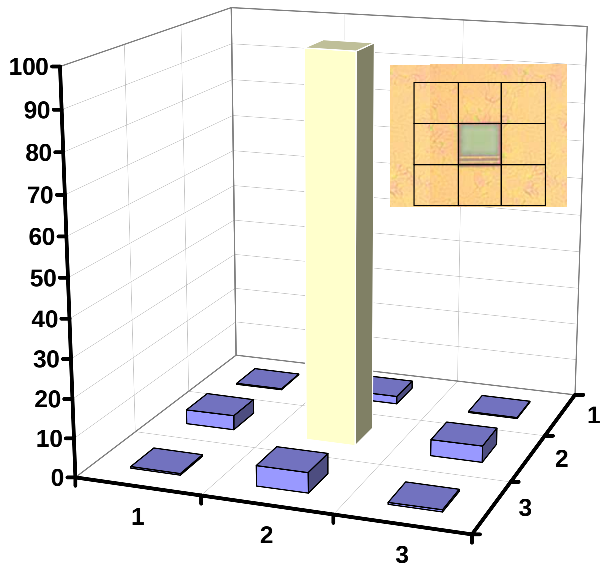


Figure 13 : Block response at 800nm

Significant signal is only obtained on the surrounding pixels. As can be seen, crosstalk increases with the wavelength and seems to be asymmetrical. The figure 14 shows more precisely the wavelength dependence and the differences between the pixel responses.

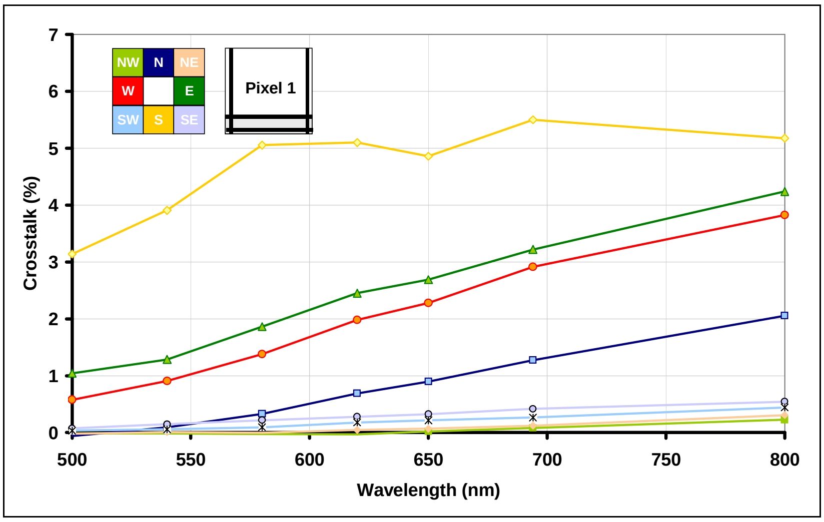


Figure 14 : Crosstalk evaluation on the pixel block in which the central pixel is totally unmasked

We can notice that the values measured on the W-pixel and the E-pixel are very close and that crosstalk varies quasi linearly with wavelength. Even at long wavelength, for which diffusion is very important, crosstalk values are low, thus proving the good performances of this technology for imaging applications. Regarding the curves obtained for the N-pixel and the S-pixel, crosstalk appears clearly as being asymmetric.

Similar quasi-linear trends have already been found by simulation and measurements on CCD test structures [5] as on CMOS pixels [6] by photocurrent calculations. This last work showed also evident differences between crosstalk values depending on the diffusion direction. Measurements made on four CMOS image sensors (including two commercial sensors) revealed an equivalent asymmetry [7].

It is now interesting to wonder why, while the diffusion phenomenon is isotropic, the crosstalk does not show a symmetry. The study of pixel kernels n°9 to n°13 would allow us to get a better knowledge of transistors area participation to crosstalk, and more particularly to the relative response of the S-pixel (figure 15).

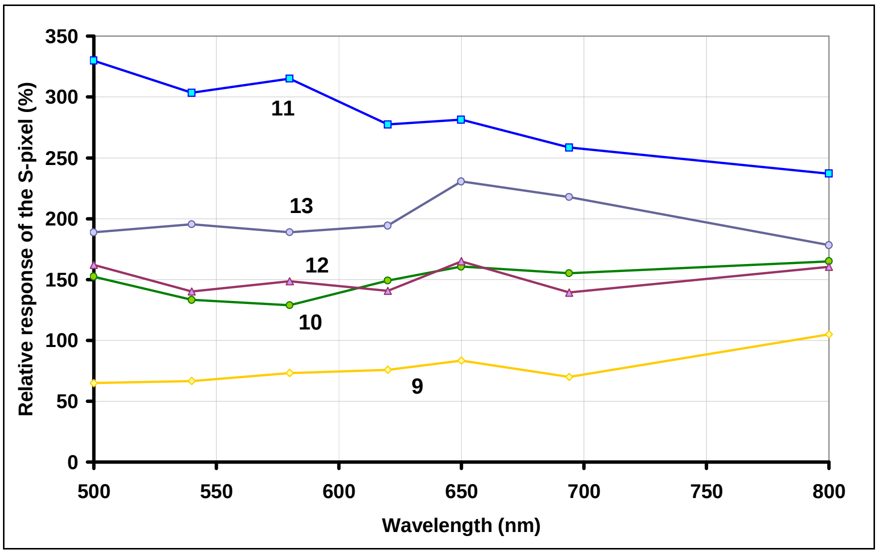


Figure 15 : Relative response of the S-pixel with regard to the central one on which only a part of transistors area is uncovered

In pixel blocks n°10 to n°13, the S-pixel response is higher than the one of the central pixel for all wavelengths. By analyzing the pixel layout, it seems that the geometric repartition of areas containing only Field Oxide (no metal lines, no transistors) could explain the differences in crosstalk values.

### 4.3. Modulation transfer function

Modulation Transfer Function measurements have been made using the slanted-edge pattern implemented at the chip level. Results have been validated by sine target and slanted-edge target measurements [8].

Figures 16 and 17 show the MTF in the row and the column direction, measured for four wavelengths between 500nm and 800nm. The integration MTFs, calculated applying a two-dimensional Fast Fourier Transform to the photosensitive area shape [9], are also shown.

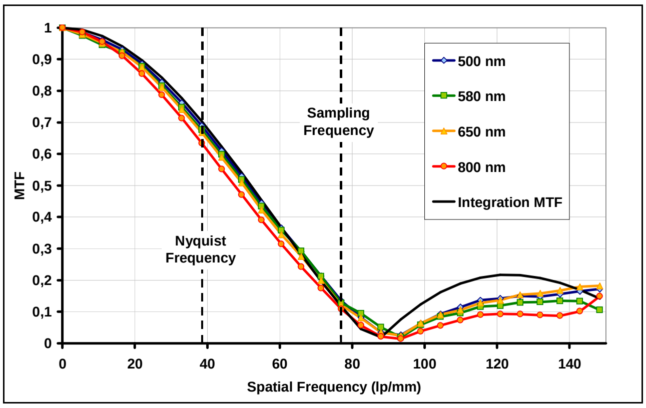


Figure 16 : MTF in the row direction (X)

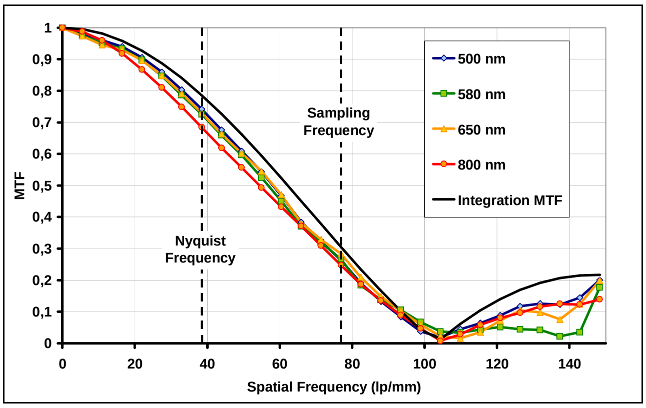


Figure 17 : MTF in the column direction (Y)

The photosensitive area is of course smaller than the pixel. Thus explains that the MTF cutoff frequency is higher than the sampling frequency. The photosensitive area has a rectangular shape, larger in the row direction than in the column one. So, the Y MTF must theoretically be better than the X MTF. The following table presents values obtained at the Nyquist frequency (half the sampling frequency) for the integration and the measured MTFs.

| | MTF X | MTF Y |
|---|---|---|
| Integration MTF | 0.70 | 0.79 |
| 500 nm | 0.69 | 0.74 |
| 580 nm | 0.68 | 0.73 |
| 650 nm | 0.67 | 0.73 |
| 800 nm | 0.63 | 0.68 |

As expecting, the Y MTF is better than the X one. We can notice that measured MTFs are very close to the integration MTF, particularly in the row (X) direction. Higher crosstalk values obtained in the column (Y) direction can explain the larger difference between integration and measured MTF.

Spotscan measurements allow us to confirm that the spatial photoresponse contribution do match the photosensitive area shape. They have been made with an optical spot (about 1.5µm diameter at 500nm) obtained using a point source associated with a microscope objective. The figure 18 presents measurements made in the horizontal and the vertical direction.

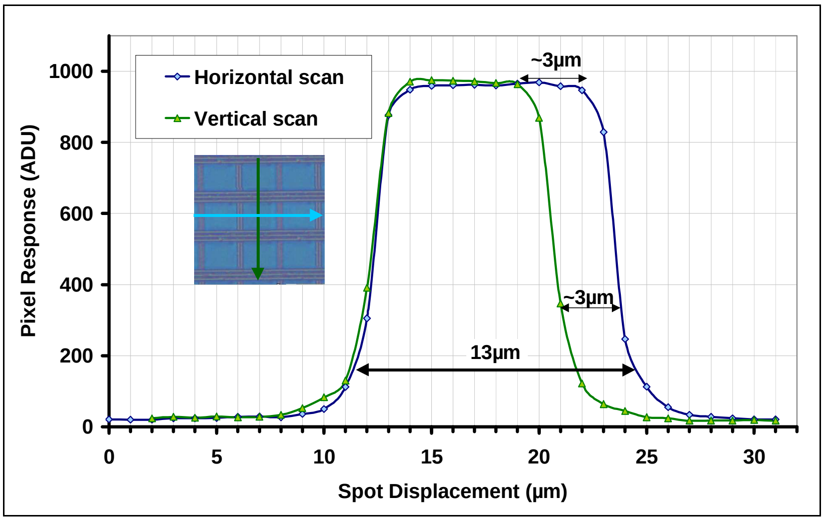


Figure 18 : Spotscan measurements on the 13µm pitch pixel (500nm)

The 3-µm annotated on the figure corresponds to the dimension of the transistors area in the Y direction. The edges sharpness allows us to confirm that the integration MTF, only taking in consideration the photosensitive area shape, is a good approximation of the sensor MTF at short wavelengths.

## 5. SOLUTIONS FOR MEASUREMENT ACCURACY ENHANCEMENT

The pixel organization studied yields to a non-symmetrical crosstalk in the column direction. This may be problematic in centroiding and imagery applications. More, the complicated form of the PRF due to the transistors area implies that :

$$PRF(x, y) \neq PRF(x) \times PRF(y)$$

In others terms, considering the figure 18, the PRF obtained in the Y direction for example is depending on the exact position of the spot in the X direction. Thus yielding to :

$$\begin{cases} MTF(\nu_x) \neq TF[PRF(x)] \\ MTF(\nu_y) \neq TF[PRF(y)] \end{cases} \quad \text{and} \quad MTF(\nu_x,\nu_y) \neq MTF(\nu_x)\times MTF(\nu_y)$$

Thus yields to difficulties in measurements to get the 2D MTF. The simplest solution is to apply the 2D Fourier Transform to the PRF but this one must be correctly sampled with a very small spot to give correct MTF results. More, for easiest image deconvolution process, it is preferable to have a symmetrical PRF, thus implies at least a symmetrical crosstalk.

### 5.1. Transistors area masking

In order to quantify the participation of the entire transistors area to the crosstalk, we study the block containing the pixel n°2 (transistors area totally covered by the upper metal layer). Figure 19 shows the responses of the pixels surrounding the pixel n°2.

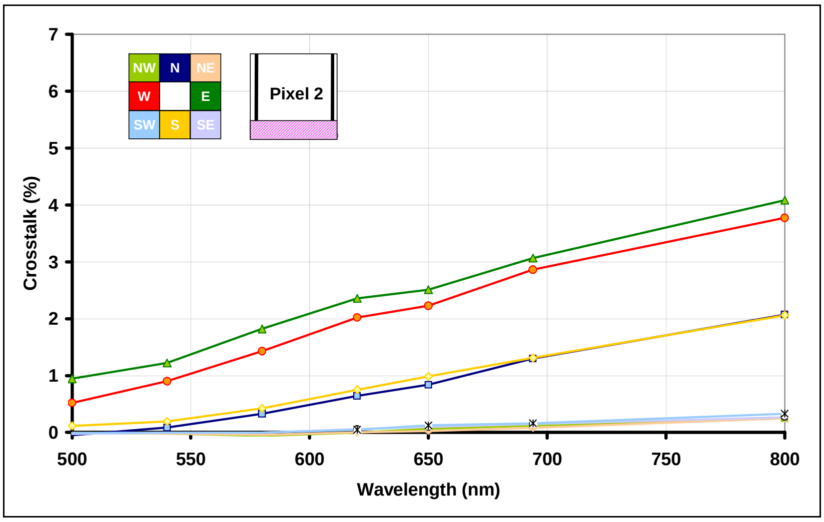


Figure 19 : Crosstalk evaluation on the pixel block in which the central pixel transistors area is totally masked

While the crosstalk values are unchanged in the horizontal direction (W-pixel and E-pixel), transistors area masking reduces crosstalk calculated on the S-pixel. More, values obtained for the S-pixel and the N-pixel are the same so crosstalk is now symmetric.

Masking the pixels transistors area seems to be a great solution for obtaining a symmetrical crosstalk (for each direction) and lower values. As crosstalk is reduced, the MTF (particularly the column MTF) is increased, thus yielding to a better accuracy for imaging applications. In order to verify crosstalk reduction and symmetrization influence on centroiding applications, we have calculated the error in centroid estimate with regard to the position of the spot (gaussian input, FWHM = 1 pixel). Three configurations have been used : the first with zero crosstalk, the second with with crosstalk values measured on pixels kernel n°1 (at 800nm) and the last with crosstalk values of kernel n°2 (at 800nm). Results are shown in figure 20.

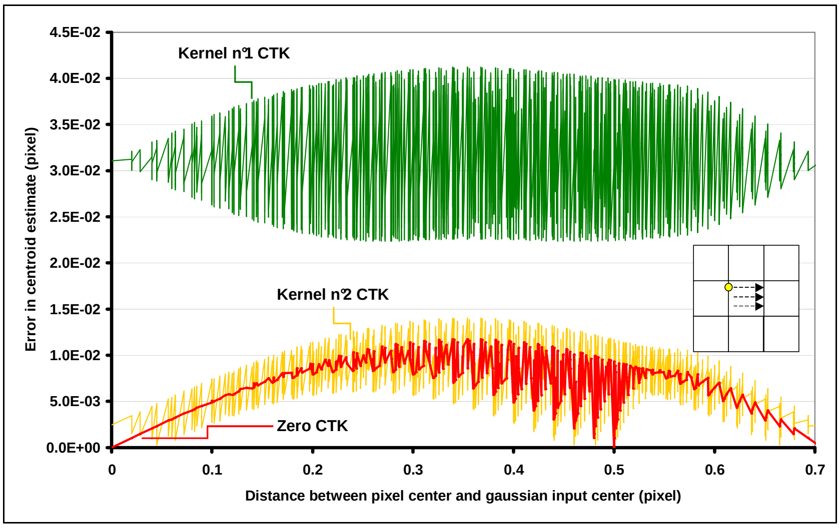


Figure 20 : Influence of crosstalk reduction and symmetrization on centroid estimation

As can be seen, the most important error in centroid estimate is obtained for the kernel n°1, i.e. when crosstalk is non-symmetrical. The positionnal shift error $\sigma_{position}$ is about 0.0057 pixel for kernel n°1 when it is only about 0.0025 pixel for zero crosstalk. Masking active area allows to obtain $\sigma_{position}$ = 0.0029 pixel, so nearly the results obtained with zero crosstalk.

We can also imagine the systematic masking of any part of the pixel which is not designed to be photosensitive. This solution has already been studied for interline CCDs [10] and for CMOS pixels [11][12]. We can expect an additionnal reduction of crosstalk, which may yield to better accuracy measurements.

In our case, as shown previously in figure 9, masking the transistors area does not affect severely affect the pixel quantum efficiency so the signal to noise ratio (SNR) will not be very affected. However, this parameter must be taken into account when using a technology for which transistors area participation to the pixel signal is more significant [13]. In this particular case, masking may reduce accuracy in terms of aperture photometry measurements.

### 5.2. Layout optimization

The general pixel organization must be chosen with regard to the applications. Three pixel designs (photosensitive area shapes) are commonly used : square, rectangular or L-shaped. For a given pixel pitch, the L-shaped pixel generally allows to reach a higher fill-factor than the square and the rectangular shaped pixel. So it may have a better quantum efficiency. However, due to their more regular shape, the two others design would be easier to use in a centroiding algorithm.

In an attempt to reduce and symmetrize crosstalk while preserving the transistors area capacity to integrate the incident light and so the SNR, the pixel layout can be optimized. We have seen that the geometry of the transistors area (so the transistors and metal lines repartition) may explained the dissymmetry of the crosstalk map. The design rules do not allow to place elements anywhere in the transistors area. However, it is possible to tend towards a minimization of remaining naked areas initially situated in the close proximity of the neighbor pixel or a symmetrization of crosstalk through appropriate design organization.

## 6. CONCLUSION

This work allows us to bring up the transistors area participation to pixel response (quantum efficiency) and to crosstalk. Thanks to an optimized technology, collection efficiency of the photodiode is clearly better than the one of the transistors area. Due to this fact, participation of the active area to pixel response is limited and the photosensitive area shape is preponderant in PRF. So, the sensor MTF can be evaluated by integration MTF at short wavelengths.

Crosstalk varies quasi-linearly with wavelength but presents a dissymmetry mostly due to transistors area organization, degrading measurements accuracy in imagery and centroiding applications. Masking transistors area appears as a good solution to reduce crosstalk by recovering a symmetry and without an important loss in quantum efficiency. However, in order to keep the photosensitive capability of the transistors area for photometry applications, it may be possible to optimize the pixel layout and particularly the transistors area.


## ACKOWLEDGMENTS

The authors want to thank Franck Corbière and Céline Engel (Supaero Integrated Image Sensors Laboratory) respectively for their help in designing the test array and for the spotscan measurements. Thanks to EADS Astrium for its financial and technical support (especially Olivier Saint-Pé and Bertrand Calvel).


## REFERENCES


1. A.Piterman, Z.Ninkov, "Subpixel sensitivity maps for a back-illuminated charge-coupled device and the effects of nonuniform response on measurement accuracy", Optical Engineering,, Vol.41, n°6, June 2002, pp 1192-1202.
2. D.Kavaldjiev, Z.Ninkov, "Influence of nonuniform charge-coupled device pixel response on aperture photometry", Optical Engineering,, Vol.40, n°2, February 2001, pp 162-169.
3. D.Kavaldjiev, Z.Ninkov, "Subpixel sensitivity map for a charge-coupled device sensor", Optical Engineering,, Vol.37, n°3, March 1998, pp 948-954.
4. International Standard ISO 12233:2000(E)
5. J.P.Lavine, W-C.Chang, C.N.Agnastopoulos et al., "Monte Carlo Simulation of the Photoelectron Crosstalk in Silicon Imaging Devices", IEEE transactions on Electron Devices, Vol.32, n°10, October 1985, pp 2087-2091.
6. H.Mutoh, ,"3-D Optical and Electrical Simulation for CMOS Image Sensor", IEEE transactions on Electron Devices, Vol.50, n°1, January 2003, pp 19-25.
7. J.S.Lee, M.E.Jernigan, R.I.Hornsey, ,"Empirical Characterization of Lateral Crosstalk for CMOS Image Sensors and Deblurring Operations", IEEE workshop on Charge-Coupled Devices and Advanced Image Sensors, Elmau, Allemagne, 15-17 May 2003.
8. M.Estribeau, P.Magnan, " Fast MTF measurement of CMOS imagers at the chip level using ISO 12233 slanted-edge methodology ", SPIE Remote sensing 2004, Proceeding of SPIE, Vol.5570, September 2004.
9. O.Yadid-Pecht, "Geometrical modulation transfer function for different pixel active area shapes", Optical Engineering,, Vol.39, n°4, April 2000, pp 859-865.
10. A.Toyoda, Y.Suzuki, K.Orihara, Y.Hokari, ,"A Novel Tungsten Light-Shiel Structure for High-Density CCD Image Sensors", IEEE transactions on Electron Devices, Vol.38, n°5, May 1991, pp 965-968.
11. H.Mutoh, ,"3-D Optical and Electrical Simulation for CMOS Image Sensor", IEEE transactions on Electron Devices, Vol.50, n°1, January 2003, pp 19-25.
12. M.Furumiya, H.Ohkubo, Y.Muramatsu et al., ,"High-Sensitivity and No-Crosstalk Pixel Technology for Embedded CMOS Image Sensor", IEEE transactions on Electron Devices, Vol.48, n°10, October 2001, pp 2221-2227.
13. O.Yadid-Pecht, B.Pain, C.Staller, C.Clark, E.Fossum, "CMOS Active Pixel Sensor Star Tracker with Regional Electronic Shutter", IEEE Journal of solid-state circuits, Vol.32, n°2, February 1997, pp 285-288.